Chapter

Trailing Edge Bluntness Noise Characterization for Horizontal Axis Wind Turbines [HAWT] Blades

Satya Prasad Maddula, Vasishta Bhargava Nukala,
Swamy Naidu Neigapula Venkata,
Chinmaya Prasad Padhy and Rahul Samala

Abstract

Wind turbine noise is becoming a critical issue for many offshore and land-based wind projects. In this work, we analyzed trailing edge bluntness vortex shedding noise source for a land-based turbine of size 2 MW and blade span of 38 m using original Brooks Pope and Marcolini (BPM)and modified BPM noise model. A regression-based curve fitting approach has been implemented to predict the shape function in terms of thickness to chord ratio of aerofoils used for blade. For trailing edge height of 0.1% chord, computations for sound power level were done at wind speed of 8 m/s, 17 RPM. The results showed that present approach for thickness correction predicts the noise peak of ~78dBA at f ~ 10 kHz which is ~15dBA lower than that predicted from original BPM. The results were also validated using experiment data from GE 1.5sle, Siemens 2.3 MW turbines with blade lengths between 78 m and 101 m which agreed within 2% at high frequencies, f > 5 kHz. In addition, results from present approach for trailing edge bluntness noise agreed well with modified BPM by Wei et al. at high frequencies, f ~ 10 kHz where it becomes dominant. The slope of noise curves from present approach, and modified BPM methods are lower when compared with original BPM.

Keywords: Noise, blades, trailing edge, turbulent boundary layer, sound power

1. Introduction

Wind power is growing at exponential rate with installed wind power capacity reached more than 500 GW globally. By far the cheapest source of energy generation among all renewable energy technologies is wind power. As more wind power projects are installed, a growing concern of noise emissions from wind turbine blades is increasing due to adverse health effects on inhabitants living near wind farms [1]. Many policy makers are considering this issue seriously as noise generated from wind turbines is an impediment to the growth of wind energy growth. Modern megawatt scale turbines have large rotor diameter of size 100 m and above which contribute to the overall noise levels and cause annoyance for people living near wind farms. **Figure 1** depicts the evolution of size of horizontal axis wind turbines over the period of forty years. Size of rotor diameter ranges from 17 m to ∼165 m with its nominal power range between 70 kW to 6 MW.

Airfoil self-noise from wind turbines with longer blades have higher tip speeds and produce high aerodynamic noise. Studies by several researchers have found that most of the broadband aerodynamic noise emissions occur due to trailing edge source from rotating blades such as from helicopter, wind turbines and compressors [2–5]. However when the blades become thicker, the trailing edge bluntness source also dominates between moderate to high frequency range in noise spectra. Airfoil self-noise prediction models developed by Brooks Pope and Marcolini (BPM) have been studied and improved by several researchers [6–8]. One of the recent improvements in the trailing edge bluntness noise predictions was done by Wei et al. (2016) who applied numerical techniques and correlated their results with field experiments measured for Siemens 2.3 MW wind turbine blade. They also used computational aero-acoustic (CAA) method to compute the trailing edge bluntness noise level from NACA 0012 airfoil with finite thickness for consistent validation of results obtained from BPM semi empirical noise prediction model and measured noise data. In addition, NACA 63–418 with two different variants of trailing edge shapes were studied to compare the noise spectra. They modified the generalized shape function proposed by original BPM model and made it independent of the solid angle formed between the trailing edge surfaces of airfoil to investigate the effect of the shape function on the trailing edge tonal noise peak produced in the high frequency region of sound spectra. In the present study, we investigate the shape function used by BPM model for predicting the trailing edge bluntness noise source but also apply regression approach to improve the bluntness peak at the high frequency region of noise spectra. To the best of authors knowledge, regression approach has not been implemented before to study the effects of trailing edge tonal noise source for wind turbine blades. In Section 2, we describe the trailing edge bluntness noise method developed by BPM along with present formulation. In Section 3, geometry model of wind turbine blade used in study is described along with IEC 61400–11 standards for measurements of acoustic emissions for wind turbines. Computational assumptions are described for the generating aerodynamic flow field by means of BEM which is coupled to the noise solver for predicting sound power level. The noise solver for the trailing edge bluntness source is

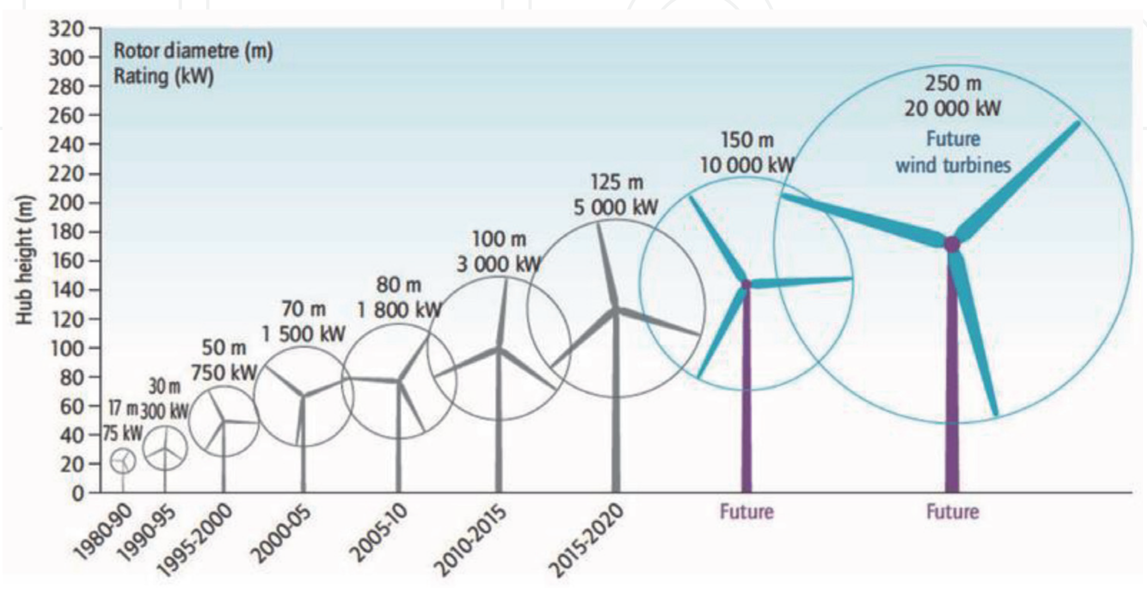

Figure 1.
Illustration of size of horizontal axis wind turbines (HAWT) and its evolution over a period of forty years.

developed based on the original BPM model along with its improvements proposed by [9]. Regression method is then applied on trailing edge noise shape function based on the coefficients obtained for the modified trailing edge height of the airfoils along the span wise direction of blade. In Section 4, present results for trailing edge bluntness noise source are compared to those obtained from original BPM, modified BPM by [9]. Overall 1/3rd octave band sound power level for the 2 MW wind turbine with a blade length of 38 m are computed and validated with experiment data of the GE 1.5sle, Siemens SWT 2.3 MW with 93 m, 95 m, and 101 m versions of turbines. Finally, conclusions are presented based on the results obtained for the original BPM, modified BPM and present correction function for airfoil thickness to chord ratio.

2. Methods

2.1 BPM model: trailing edge bluntness vortex shedding

Flow around wind turbine blades can be considered often as incompressible and low Mach number for most utility scale wind turbines. Even though they operate in environments where the effects of air density and wind shear on power production are significant, aerodynamic noise generation from wind turbine blades becomes important when the blade tip speed range between 0.1 and 0.3 Mach number. As length of blade is increased, the sound radiation from blades depends not only upon aerofoil geometry, local angle of attack for the aerofoils but also the rotational speed of rotor. One of the noise mechanisms from blades occurs due to periodic vortex shedding from suction side of trailing edge surface when the turbulent boundary layer flow interacts with blade surface and contributes to a monotonic peak in high frequency region of noise spectrum. For a given flow condition i.e., Reynolds number and Mach number along the span wise direction of the blade strongly affects the overall noise levels as well as the tonal noise production. Typically, the noise amplitudes increase with increase in flow Mach number and Reynolds number of order 8×10^6.

Vortex shedding is aerodynamic phenomenon observed on both streamlined and bluff bodies such as an aerofoil or a cylinder and becomes dominant when there exists an adverse pressure gradient within the boundary layer which causes a relative difference in the flow velocities between the surface and free stream flow conditions. According to BPM model, the trailing edge vortex shedding occurs when the turbulent boundary layer displacement thickness is at least 30% higher than characteristic dimension of source [6, 10]. In addition, flow conditions such as angle of attack, Reynolds number and Mach number affect the aerodynamic lift and drag force characteristics of an aerofoil. It can be noted that for low angle of attack and attached flows, vortex shedding from trailing edge occurs rapidly and produces unsteady lift which often result in higher noise generation [11]. The lift and drag coefficient at high angle of attack also increases rapidly but reach maximum values near stall angle of attack. For aerofoils with finite trailing edge thickness, and at stall angle of attack, the vortex shedding phenomenon is reduced due to turbulent boundary layer separation near the trailing edge. Beyond the stall angle of attack, significant reduction of lift can be observed and hence vortex noise from aerofoils is also reduced. BPM model predicts noise radiation from aerofoils using relative velocity and angle of attack as primary inputs and computes the turbulent boundary layer data for suction and pressure sides of aerofoil. This data varies according to the thickness of trailing edge of aerofoil as well as the chord length of aerofoil. As the thickness to chord increases, the turbulent boundary layer on the suction side of aerofoil becomes less stable and tend to shed vortices rapidly. For a rotating wind turbine blade, the vortex shedding occurrence happens at faster rate which leads to the massive flow separation near the tip of blade due to centrifugal force action on the flow. The separated flow appears as wake which has lower velocity compared to free stream flow condition and contributes to aerodynamic noise. Further, according to this method, the strength of this source is approximated using the spectral functions, G_4 and G_5 which are functions of ratio of trailing edge thickness and average turbulent boundary layer displacement thickness from pressure and suction sides of aerofoil as given by Eq. (5). Hence, it is needed to compute the spectral functions G_4 and G_5 as given by Eq. (6)–(8). G_4 represents the narrowband peak in spectra and G_5 is used to determine the broadband overall shape of spectra which is dependent on Strouhal number, St''' and St_{peak}'''.

The two spectral functions $(G_5)_{\varphi\,=\,14}$ and $(G_5)_{\varphi\,=\,0}$ are solid angles which are determined using the symmetric NACA 0012 aerofoil experiments and given by Eq. from (76) to (82) in (Brooks et al., 1989). As mentioned by [6, 10], the bluntness vortex shedding source appears as tonal peak in the overall noise spectra and becomes dominant near 10 kHz masking other self-noise mechanisms. It must be noted that the functional parameters in Eq. (1) are expressed in terms of the flow angle of attack, bluntness ratio h/δ^*, for aerofoil at moderate to high Reynolds number; at the same time, they show the dependence of Mach number, $M^{5.5}$. The noise levels are also found to vary with the span segment length of aerofoil, L and inverse square of the distance between source and receiver, r^2_e as given in Eq. (1). The Strouhal number for this type of source is defined according to Eq. (2) where h is the height of trailing edge. It must be noted that at moderate Reynolds number and for subsonic Mach number flows, the chord Reynolds number and turbulent boundary layer thickness and displacement thicknesses for zero and non-zero angle of attack are evaluated using Eq. (5) and Eq. (16) given in [6]. The 1/3$^{\text{rd}}$ octave sound pressure for this source is approximated using the Eq. (1). The narrowband tonal peak is given by function G_4 and expressed using Eqs. (6) and (7).

Function G_5 is calculated using ratio of trailing edge thickness to average boundary layer displacement thickness and sloping angle, φ between 0° to 14° given by Eq. (78) and Eq. (79) found in [6] where φ is the angle between the sloping surfaces near trailing edge of aerofoil and δ^*_p and δ^*_s are the pressure and suction side turbulent boundary layer displacement thickness, and h is the trailing edge height. The empirical equations used to determine the pressure and suction side displacement thicknesses for zero and non-zero angle of attack for symmetric aerofoils are given in [6]. They are found to be dependent upon the local angle of attack and chord Reynolds number. For an aerofoil, it is expressed in terms of the turbulent boundary layer displacement thicknesses for the pressure and suction side. This source also uses the high frequency directivity function like turbulent boundary layer trailing edge noise and given by the Eq. (9).

$$SPL_{\text{Blunt}} = 10\log\frac{hM^{5.5}LD_{\text{h}}}{r_{\text{e}}^2} + G_4\left(\frac{h}{\delta^*_{\text{avg}}},\varphi\right) + G_5\left(\frac{h}{\delta^*_{\text{avg}}},\varphi,\frac{St'''}{St'''_{\text{peak}}}\right), \qquad (1)$$

$$St''' = \frac{fh}{U}, \qquad (2)$$

$$St'''_{\text{peak}} = \frac{0.212 - 0.0045\varphi}{1 + 0.235\left(\frac{h}{\delta^*_{\text{avg}}}\right)^{-1} - 0.0132\left(\frac{h}{\delta^*_{\text{avg}}}\right)^{-2}}, \quad \text{for } \frac{h}{\delta^*_{\text{avg}}} \geq 0.2, \qquad (3)$$

$$St'''_{\text{peak}} = 0.1\left(\frac{h}{\delta^*_{\text{avg}}}\right) + 0.095 - 0.00243\varphi, \quad \text{for } \frac{h}{\delta^*_{\text{avg}}} < 0.2, \qquad (4)$$

$$\delta^*_{\text{avg}} = \frac{\delta^*_{\text{p}} + \delta^*_{\text{s}}}{2}, \tag{5}$$

$$G_4\left(\frac{h}{\delta^*_{\text{avg}}}, \varphi\right) = 17.5 \log \frac{h}{\delta^*_{\text{avg}}} + 157,5 - 1.114\varphi, \quad \textit{for} \ \frac{h}{\delta^*_{\text{avg}}} \le 5, \tag{6}$$

$$G_4\left(\frac{h}{\delta^*_{\text{avg}}}, \varphi\right) = 169.7 - 1.114\varphi, \quad \textit{for} \ \frac{h}{\delta^*_{\text{avg}}} > 5, \tag{7}$$

$$G_5\left(\frac{h}{\delta^*_{\text{avg}}}, \varphi, \frac{St'''}{St'''_{\text{peak}}}\right) = (G_5)_{\varphi=0^\circ} + 0.0714\varphi\left[(G_5)_{\varphi=14^\circ} - (G_5)_{\varphi=0^\circ}\right], \tag{8}$$

$$D_H(\theta, \phi) = \frac{2\sin^2(1/2\theta)\sin^2\phi}{(1 + \text{M}\cdot\cos\theta)[1 + (\text{M} - \text{M}_\text{C})\cos\theta]^2}, \tag{9}$$

where θ, ϕ are the directivity angles between the source and receiver line aligned to blade span and chord direction with respect to the receiver position. M is the Mach number and M_c is the convective Mach number. h, is the trailing edge height. The denominator term in Eq. (9) represents the Doppler effect and convective amplification of acoustic waves produced at the trailing edge of aerofoil [6, 10, 12, 13]. It has been proven that for high values of Strouhal number or for the order greater than 2, the flow is dominated by turbulent boundary layer thickness and results in small scale flow instabilities [6, 14–16].

The Strouhal number and the shape functions vary with the shape of aerofoil, inflow velocity conditions and local angle of attack. Experiments conducted by [6] used a reference chord length for test aerofoil which was 30.86 cm and boundary tripping was done with help of 2 cm wide strip or grit applied at 15% chord length. Tripping of boundary layer resulted in reduction of the noise levels in certain frequency regions of sound spectrum [7, 8, 17]. For the present analysis, tripping of turbulent boundary layer has not been taken into consideration.

The maximum trailing edge height in BPM model aerofoil experiments was 2.5 mm which is ~0.8% of chord. For the present case of 38 m blade, it is 32.2 mm and corresponds to 1% chord, respectively.

2.2 Shape function and trailing edge thickness approximation proposed by Wei et al

As mentioned previously, trailing edge bluntness vortex shedding model was developed based on the experiment data obtained from NACA 0012. To account for the effects of vortex shedding noise levels, the geometry near the trailing edge requires an interpolation function essentially to approximate the height of trailing edge sloping surfaces. Standard solid angle was specified as ψ = 14° for a NACA 0012 aerofoil while for a flat plate it is ψ = 0°. However, it must be noted that a wind turbine blade has finite thickness and varying camber along span direction. This led to erroneous predictions of the trailing edge noise levels. Hence [9] used a modified interpolation function for the trailing edge bluntness noise source and corrected the Eq. (1) using two additional functions viz. S_1 and S_2. S_1 is the shape function that is equivalent to the actual G_5 function and S_2 is the correction function for aerofoil thickness variation along the span wise direction of the blade given by Eqs. (10) and (11)

$$SPL_{\text{Blunt}} = 10\log_{10}\frac{hM^{5.7}LD_h}{r_e^2} + 20\left(1+M^2\right)\log_{10}\left(\frac{h}{\delta^*{}_{avg}}\right) + S_1\left(\frac{h}{\delta^*{}_{avg}}, \frac{St}{St_{peak}}\right) + S_2\left(\frac{t}{c}\right) + K_0 \tag{10}$$

$$S_2 = 654.43\left(\frac{t}{c}\right)^3 - 652.26\left(\frac{t}{c}\right)^2 + 58.77\left(\frac{t}{c}\right) \tag{11}$$

Where, the constant, K_o is taken as 150 for $h/\delta^* < 0.2$ otherwise K_o is approximated as $150–20(h/\delta^* -0.2)^{0.25}$. The Eq. (10) was modified in such a way that noise levels are not dependent of the solid angle formed at the trailing edge surfaces rather expressed as function of the bluntness height *h,* Mach number, *M,* and average of the boundary layer displacement thickness between suction and pressure sides of airfoil, δ^*_{avg}. Further, in the modified BPM for trailing edge bluntness, the sound pressure level is proportional $M^{5.7}$ instead of $M^{5.5}$. This change also demonstrates that the sound pressure for trailing edge bluntness source is sensitive to flow Mach number increments.

2.3 Modified thickness approximation using regression curve fitting

In the present study the basic shape function for the trailing edge angle is taken as from the original BPM model. However, for the shape function, G_5 the trailing edge angle is varied continuously between the blade root and tip section to account for differences in blade geometry. Since, the trailing edge sloping surfaces are proportional to the trailing edge height, a change in trailing edge angle parameter is retained in present noise computations while correction function for airfoil thickness, S_2 is modified in terms of thickness to chord ratio for each span segment of the blade similar to that proposed by [9]. One must note that coefficients in the modified function for thickness are obtained by regression and given by Eq. (12)

$$S_2 = -0.02158\left(\frac{t}{c}\right)^3 + 0.9518\left(\frac{t}{c}\right)^2 - 13.38\left(\frac{t}{c}\right) + 61.4 \tag{12}$$

3. Simulation assumptions

In the analysis of sound pressure from wind turbine blade, generalized blade element momentum (BEM) method was used to compute the relative velocity field along the blade span. The outputs of BEM solver are relative velocity on the blade section, angle of attack, normal and tangential force coefficients on every section of blade which can be used to compute rotor loading forces and moments. The outputs from BEM solver are coupled to BPM noise prediction module for which, sound pressure level computations are done at a given wind speed, blade pitch angle and rotational speed of the machine.

In the BEM approach the total length of blade is discretized into several aerofoils at least 20 segments. Aerofoil can be assumed as half-infinite flat plate with finite thickness and aspect ratio. The flow over flat plate was assumed to be 2D incompressible and quasi uniform along the blade length which means that flow behavior does vary from one span station to another along the blade span. The overall shape of blade is approximated using selected aerofoils, viz. NACA 0012, NACA 6320 and

NACA 63215 while the turbulent boundary layer properties on suction and pressure side of aerofoils is computed from XFOIL module. The boundary layer data for aerofoil serve as input to the noise prediction module.

In the prediction of sound pressure levels, each blade segment is treated as a point source in near field and rotating blade as line source. In the far field sound prediction however, the rotor of turbine acts as point source when operating in a wind farm. Sound pressure level is thus calculated by logarithmic addition of individual sources relative to observer position. For the present simulation work, the receiver height was fixed at 2 m above the ground level and the source height was fixed at 80 m. The distance of the receiver location was set at 110 m, which is approximately the total turbine height ($HH + D/2$). This is in accordance with IEC 61400–11 regulations for measurements of acoustic emissions from wind turbines. HH is the hub height of turbine, and D is the rotor diameter in m.

A downwind scenario is considered as the worst case since sound waves bend in downward direction with respect to free stream wind and this results in amplification. Therefore, downwind receiver location is considered. The boundary conditions for the blade are Reynolds number, the angle of attack along the blade span. It is implemented to verify that blade element momentum (BEM) computed values do not exceed predefined threshold values as given in [6]. The blade pitch angle is set to 3.5° for sound pressure calculations and rotation speed for machine as 17 RPM.

3.1 Geometric model of turbine

For the assessment of trailing edge bluntness noise from horizontal axis wind turbine rotors, a geometric model for the blade has been developed using NuMAD software [18]. The software allows user to input the aerofoil data at every span wise location of the blade. **Table 1** shows the turbine design parameters along with orientation of rotor into wind.

Figure 2 shows the isometric (3D) model of the 38 m blade for the 2 MW wind turbine used for analyzing the trailing edge bluntness noise. Towards the inboard region, the airfoils have high thickness to chord ratio with at least 18% t/c as well as high camber. In the present study NACA 6320 airfoil data have been used with a

Parameter	Value
Cone angle	0°
Tilt angle	3°
Hub height	80 m
Blade Radius	38 m
Rotor speed	17 RPM
Max twist	13°
Max chord	3.22 m
Orientation	Upwind
No of blades	3
Rated power	2 MW

Table 1.
Turbine parameters for 2 MW machine.

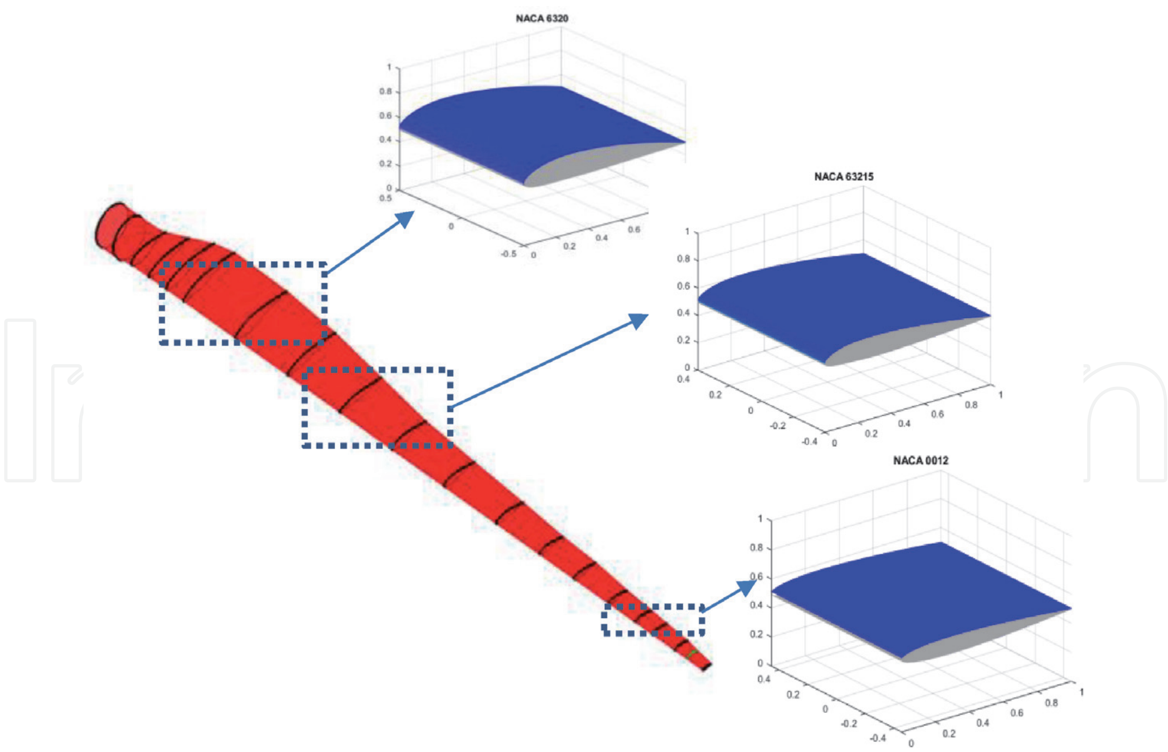

Figure 2.
Isometric (3D) model of wind turbine developed using NuMAD software showing the airfoil sections used near the blade root, mid-span, and tip of the blade [18].

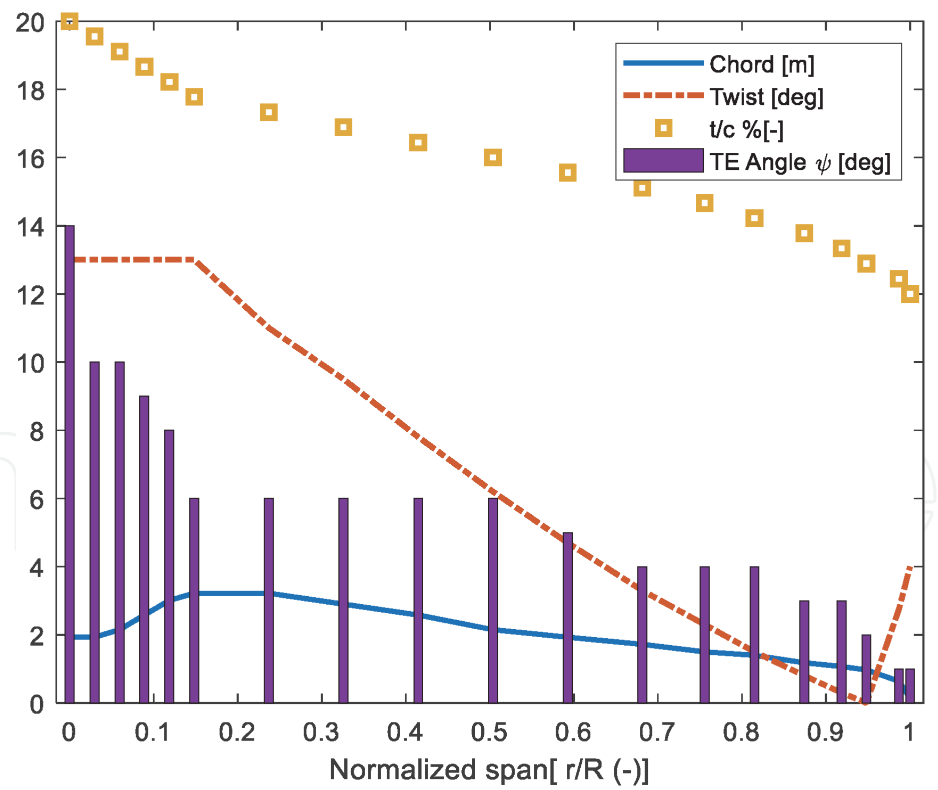

Figure 3.
Geometric properties shown along the normalized blade span for a wind turbine blade having a length of 38 m.

trailing edge slope angle of 14°. In the mid span region, the airfoils have moderate thickness to chord ratio. The geometric properties of the blade are depicted in **Figure 3**. It is evident that chord length and twist remain constant for root section which connects the blade to the rotor hub.

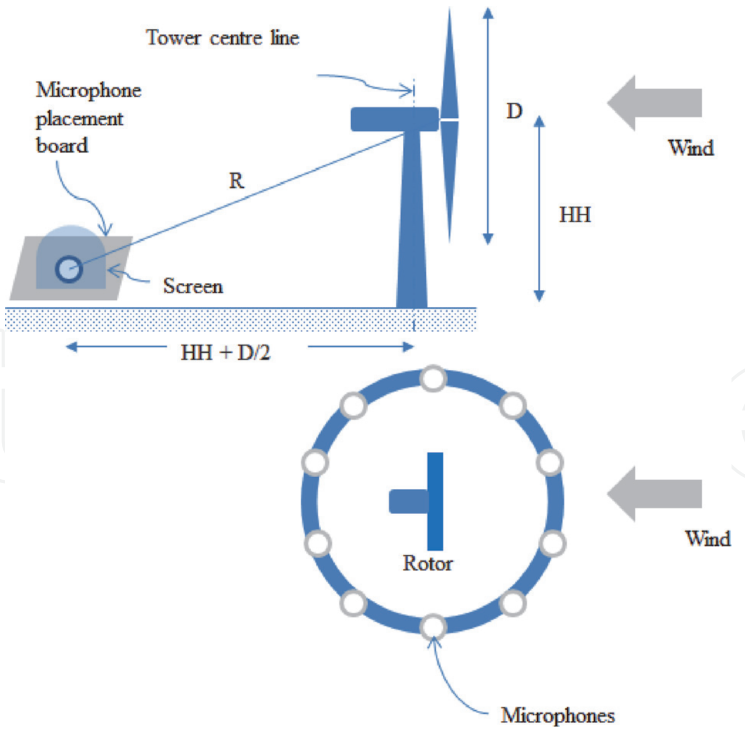

Figure 4.
Illustration of microphone position surrounding the source located in Centre as well as the microphone measurement distances and position according to IEC 61400–11 standards with respect to source.

3.2 IEC 61400-11 standard for measurement of sound level

The relative position of the receiver with respect to aerofoil coordinate system is shown in **Figure 4**. For a wind turbine blade, in addition to the turbulent boundary layer, wind speed and free stream mach number responsible for trailing edge vortex shedding noise, the sound levels also depend on blades pitch angle operation. Particularly for moderate pitch angles and at low or positive angle of attack, the boundary layer on the pressure side of aerofoil at leading edge shows laminar flow structure; however, the boundary layer on suction side remains mostly in turbulent state near the trailing edge. Further, it is important to note that such a type of noise mechanism is dominant in mid span region of blade where trailing edge thicknesses are high for which maximum Strouhal number is found to be 0.15. Below this value, the vortex shed from the trailing edge surface does not contribute significantly to the noise levels [8, 10].

4. Results and discussion

In this section we present results for the turbulent boundary layer vortex shedding noise from a 2 MW horizontal axis wind turbine blade using original BPM model predictions, modified by [9] and compare them with numerical computations implemented using the correction function for airfoil thickness. **Figure 5** illustrates the noise prediction from wind turbine blades using first order empirical methods which are based on the turbine geometric and operating parameters viz. rotor diameter, nominal power rating of machine and blade tip speed. Although such methods can predict sound power levels, they do not take account of the physical phenomenon responsible for the noise radiation from rotating blades at broadband frequencies and hence not reliable. Also, it can be said noise models proposed by [21–23] are simple algebraic functions that depend on nominal power

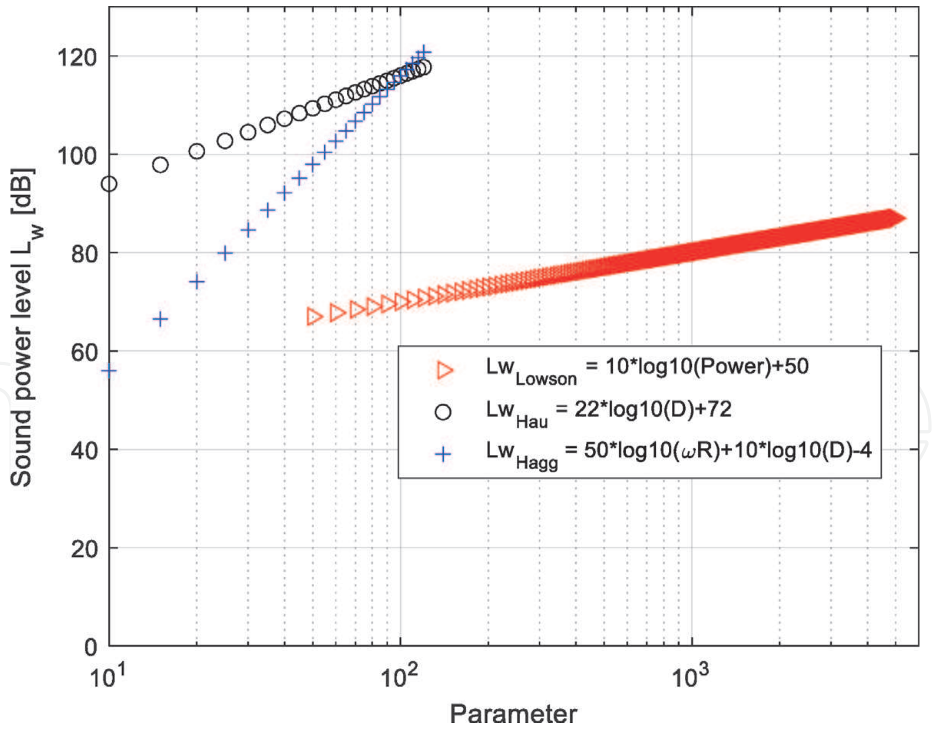

Figure 5.
Illustration of sound power level based on empirical relations proposed by [19–21].

Wind Turbine Model	dB(A)	Power (kW)	Hub Height (m)(m)	Rotor Diameter (m)
AN Bonus 600 kW/41	101.6	600	50	41
DeWind 41	99.6	500	40	41
DeWind 46	97.9	600	40	46
Enercon E-41	99	500	50	41
NORDTANK 500/41	103.2	500	50	41
SEEWIND 52–750-65	99	750	55	52
VESTAS V 66/1.65 MW	103	1650	60	66
Windtechnik-Nord 200/26	101	200	40	26

Table 2.
Sound power level, L_{wA} for utility scale commercial wind turbine models.

rating of the machine, rotor diameter and blade tip speed only. Sound power predictions from [22, 23] agree well for rotor diameters that range between 10 m and 100 m and thought to be less conservative compared to actual or measured data. Similarly, Lowson's empirical equation make use of only nominal power rating of machine, which implies that sound power level varies with size of machine. Hagg (1992) also developed a slightly more sophisticated model which can predict sound pressure level based on the axial thrust force coefficient, rotor swept area and the number of blades in machine along with empirical constants given in [21]. However, the model does not predict sound power levels for broadband frequency range of noise spectra. Some advanced noise prediction simulation software's developed by Siemens XNoise, NREL's NAFNoise are useful tools which can predict the noise levels for utility scale wind turbines. **Table 2** shows the measured sound power level (PWL) for some of commercial wind turbine models taken from SoundPLAN software.

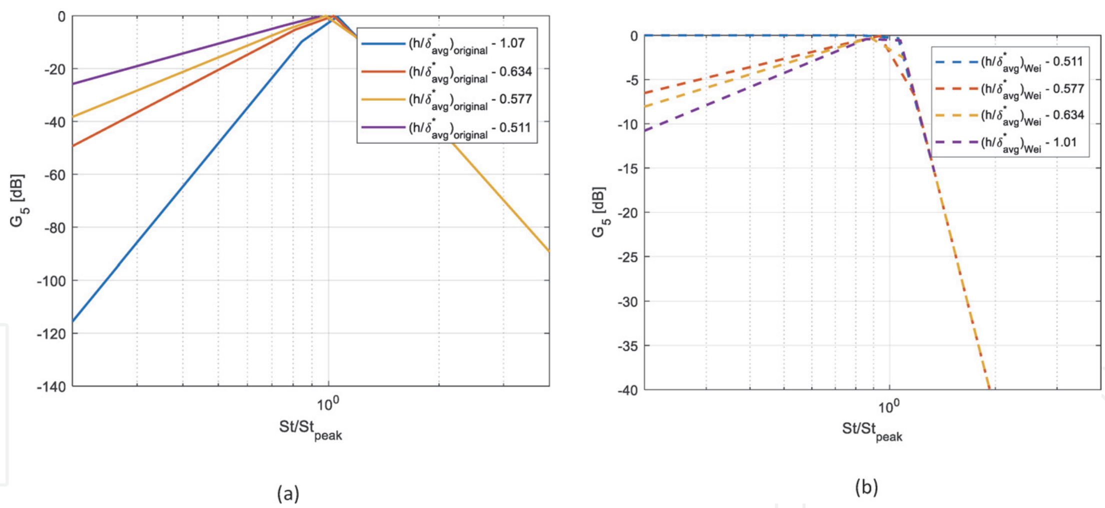

Figure 6.
Shape function, G_5, computed for different trailing edge bluntness thickness, h/δ^*_{avg} using (a) original BPM [6] (b) modified BPM by [9].

Figure 6(a) depicts the results for shape function, G_5 obtained from original BPM model. As the average boundary layer displacement thickness is reduced, the frequency of vortex shedding increased despite a change in the angle of attack and flow Mach number, *M* along the blade span. This difference can be attributed to solid angle inclusion in the original BPM model which considered trailing edge sloping angle, ψ as essential condition to vortex shedding phenomenon in addition to the trailing edge height, flow Mach number and Reynolds number.

From **Figure 6(b)** the shape function G_5 modified by [9] has been computed for trailing edge height to average boundary layer displacement thickness ratios, h/δ^*_{avg} between 0.51 and 1.01. The function showed a linear change in amplitude, dB for all Strouhal numbers of ratios between 0 and 1. As the peak Strouhal number, St_{peak} is increased, one can notice that tonal peak for trailing edge bluntness was found to be increasing. This effect was also observed with numerical CAA results obtained by [9] in their study for NACA 0012 and NACA 63–418 airfoil which have ~3% camber and maximum thickness of 18%. It is important to note that CAA computations such as large eddy simulation (LES) can predict the acoustic radiation from airfoils by solving for the largest scales of turbulent flows and approximating the small scale motions. In contrast to the semi-empirical BPM model, the sound pressure level near the surface can be computed by solving the 2D-Navier–Stokes (N-S) equations that are coupled to advanced turbulence models and high accuracy computational grid schemes suitable for acoustic pressure computations [14]. Similarly, the A-weighted $1/3^{rd}$ octave band tonal noise spectra has been computed at wind speed of 6 m/s, 14 RPM having a blade pitch of 3.5°.

Figure 7(a)–(d) demonstrates the contour plot of peak Strouhal number, plotted along the blade span for various blade azimuth angles in rotor plane and for different trailing edge thicknesses computed at wind speed of 8 m/s [19]. The maximum values can be observed between 0.1 r/R and 0.75 r/R along the blade span where the thickness to chord ratio is high when the blade azimuth angle is at 300°. With increasing trailing edge thicknesses, the peak Strouhal number kept increasing from 0.13 to 0.2. This also signifies shape function, G_5 have high tonal peaks demonstrating influence of trailing edge vortex shedding from blade caused due to change in the trailing edge thicknesses.

On the other hand, the original BPM model showed a strong tonal peak effect in noise spectrum at 12% r/R where the thickness to chord ratio is found increasing. **Figure 8** shows the computed values for overall A-weighted $1/3^{rd}$ octave band sound power level for 2 MW turbine, turbulent boundary layer trailing edge noise

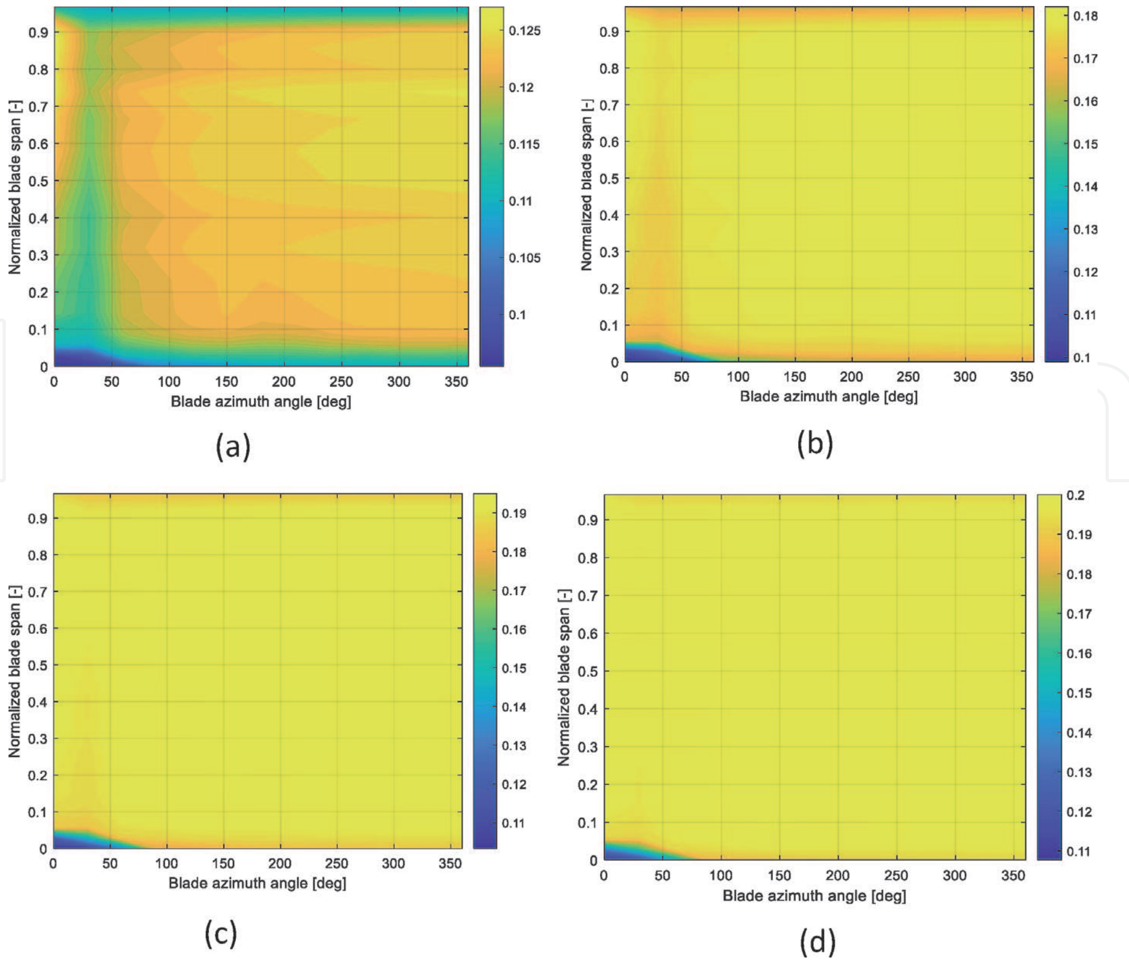

Figure 7.
Peak Strouhal number, St_{peak}''', along normalized blade span and blade azimuth angles at U = 8 m/s for TE thicknesses (a) 0.1% chord (b) 0.5% chord (c) 1% chord (d) 1.5% chord.

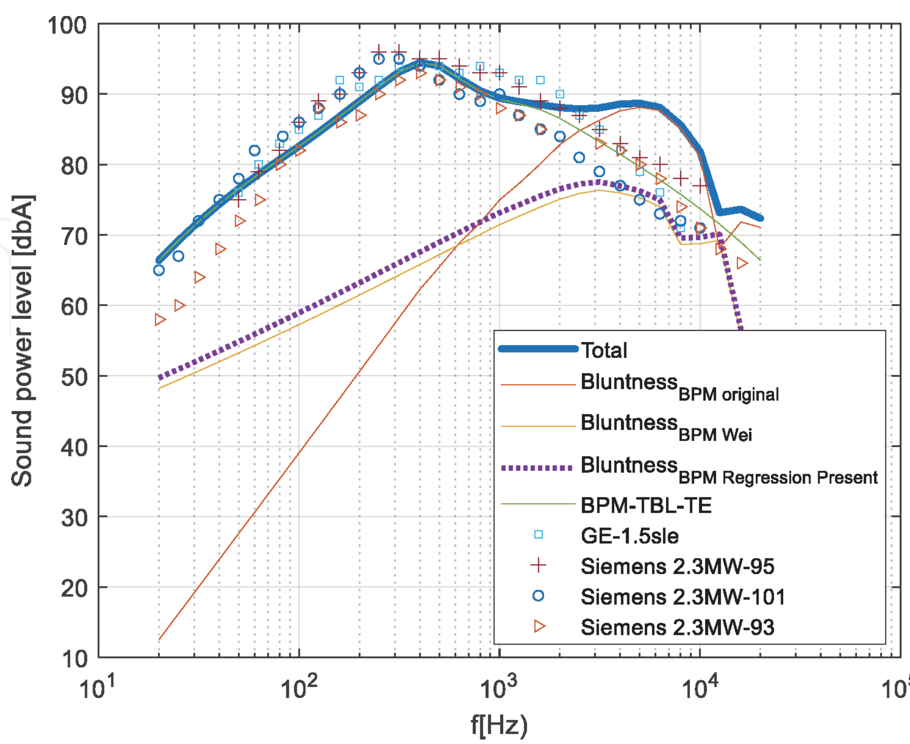

Figure 8.
Comparison of trailing edge bluntness noise using present approach to those predicted by BPM original, BPM modified [9]) and its validation with experimental data from Siemens SWT 2.3 MW and GE 1.5sle turbines at wind speed of 8 m/s for trailing edge thickness of 0.1% chord.

(TBL-TE) as well as trailing edge bluntness noise using original BPM model. All the computations were done in MATLAB 2020b software, for a wind speed of 8 m/s at blade pitch angle of 3.5° and trailing edge thickness taken ~0.1% chord length. Further, modified BPM model by [9] for trailing edge bluntness noise has also been computed to compare the actual results with present method. The present method focused on the regression approach for thickness correction along the blade span. It can be noted that present results produced similar trailing edge noise characteristics except for the noise peak change found at 10 kHz in the noise spectra. Also, one can observe that current approach for thickness correction leads to better agreement of the trailing edge bluntness peak with experiment data obtained from GE 1.5sle rather than Siemens 2.3 MW-101, Siemens 2.3 MW-95 and Siemens 2.3 MW-93 turbines. On the contrary, the trailing edge bluntness peak from original BPM model showed a broad hump which do not agree well with experiment validation data for turbines. For frequencies below 1 kHz, the turbulent boundary layer trailing edge noise dominates with a peak value of 96dBA. The trailing edge bluntness noise tonal peak computed from the original BPM model was found to be ~89 dBA. The peak trailing edge bluntness noise level for modified BPM by [9] was found to be 78 dBA near 8 kHz which agreed well with experiment data. The present computations for modified BPM showed an increase of 2 dBA for frequency range of 20 Hz and 6 kHz, but reached almost same values for frequencies, $f > 6$ kHz.

In this section we present results for the turbulent boundary layer vortex shedding noise from a 2 MW horizontal axis wind turbine blade using original BPM model predictions and compare them with OSPL (overall sound power level) experiment data obtained for GE 1.5sle, Siemens SWT 2.3 MW machines. All the computations were done in MATLAB 2020b software, for a wind speed of 7 m/s and 10 m/s at blade pitch angle of 3.5° and trailing edge thickness taken ~0.1% chord length. **Figure 9** shows the Strouhal number, *St'''* computed in terms of displacement thickness, δ^*, for wind speeds of 7 m/s and 10 m/s respectively. The maximum value for *St'''* was found to be 2.2 and 4.16 for wind speeds of 7 m/s and 10 m/s at frequency f ~ 10 kHz, where the turbulent boundary layer trailing edge bluntness noise produces peak tonal amplitude.

Figure 10(a) and **(b)** shows the trailing edge bluntness peak from original BPM model as a broad band hump that agrees well within 5% of experiment validation data for GE 1.5sle, Siemens 2.3 MW turbines for wind speed of 7 m/s and 10 m/s at

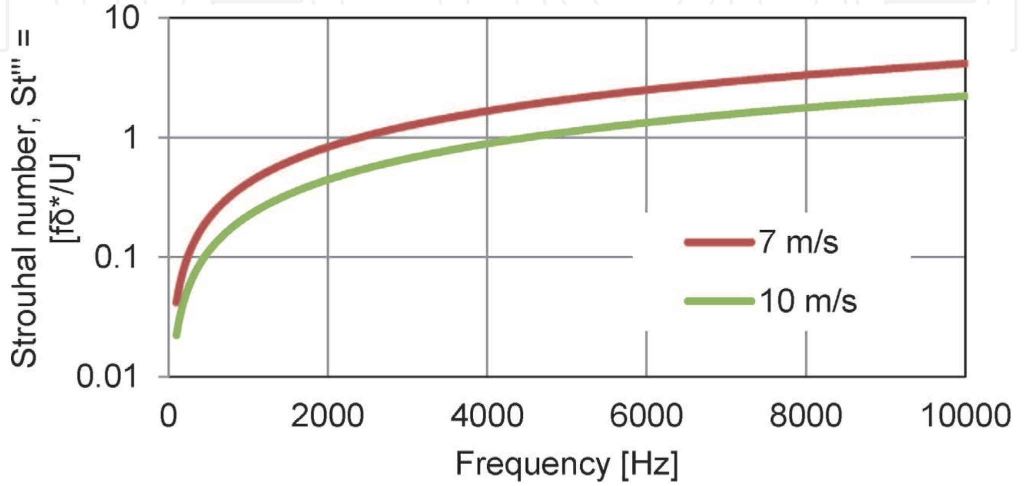

Figure 9.
Illustration of Strouhal number, St''' as function of displacement thickness, δ^*, at wind speeds of 7 m/s and 10 m/s.

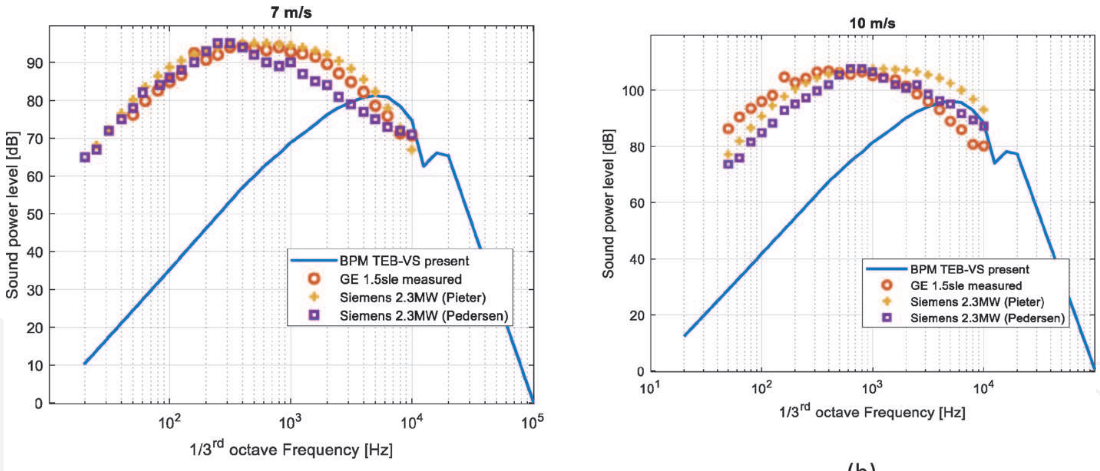

(a) (b)

Figure 10.
Validation of the computed BPM-turbulent boundary layer vortex shedding noise (TEB-VS), for a blade length of 38 m, 2 MW turbine having trailing edge thickness of 0.1%c with OSPL measured data of GE-1.5sle, Siemens 2.3 MW (Pieter), Siemens 2.3 MW (Pedersen) of blade length 47 m at two different wind speeds of (a) 7 m/s (b) 10 m/s.

trailing edge thickness of 0.1% local blade chord length. For frequencies below 1 kHz, the turbulent boundary layer trailing edge noise dominates with a peak value of 96 dB that is obtained using measured data of experiment turbines. The tonal peak of trailing edge bluntness noise computed from the original BPM model was found to be ~82 dB for wind speed of 7 m/s and 96 dB for wind speed of 10 m/s.

From **Figure 11(a)** and **(b)** one can notice the computed turbulent boundary layer trailing edge bluntness noise level using BPM model shows peaks that shift closer to frequencies, $f \sim 5$ kHz and reach an amplitude values of 97 dB and 115 dB respectively. It must be noted that when the trailing edge thickness or heights are increased to 0.5% of local blade chord length, a difference of 15 dB was found for wind speed of 7 m/s while a difference of 10 dB was obtained for wind speed of 10 m/s. Further, from **Figure 12** it is evident that the difference in the sound power levels between 7 m/s and 10 m/s continued to increase by a maximum value of 15 dB for frequencies, $f < 200$ Hz when the trailing edge thicknesses are 0.1% and 0.5% of local blade chord length respectively. However, for frequencies, $f > 200$ Hz a noise reduction of 17 dB was observed when the trailing edge thickness was 0.5% local chord length.

Figure 13 shows the measured and computed sound power level, L_{wA} for wind speeds between 4 m/s and 10 m/s. The experiment data for Vestas V82 and GE 1.5sle turbines have source heights of 80 m and blade lengths of 40 m which are nearly same as present investigated 2 MW turbine. This data is obtained for one of Vestas V82 and GE 1.5sle turbines from Jericho Rise operating wind farm located in US state of New York [20]. The results demonstrate that for wind speeds lesser than 7 m/s both experiment noise data for Vestas 82 and GE 1.5sle agree closely with each other within 1%. However, from 7 m/s to 10 m/s the sound power level remained constant which implies that there is no influence of wind speeds on sound levels which contradicts the BPM model predictions as the model is strongly dependent on Mach number. This suggests that turbines are deliberately controlled above certain wind speeds in order to regulate power. Further, the model simulated values for the present case of 2 MW turbine also agree closely with experiment data of both turbines with a peak difference of 5dBA at wind speed of 6 m/s. This shows that model can predic the sound levels accurately and reliably be used for the noise assessment of wind turbines.

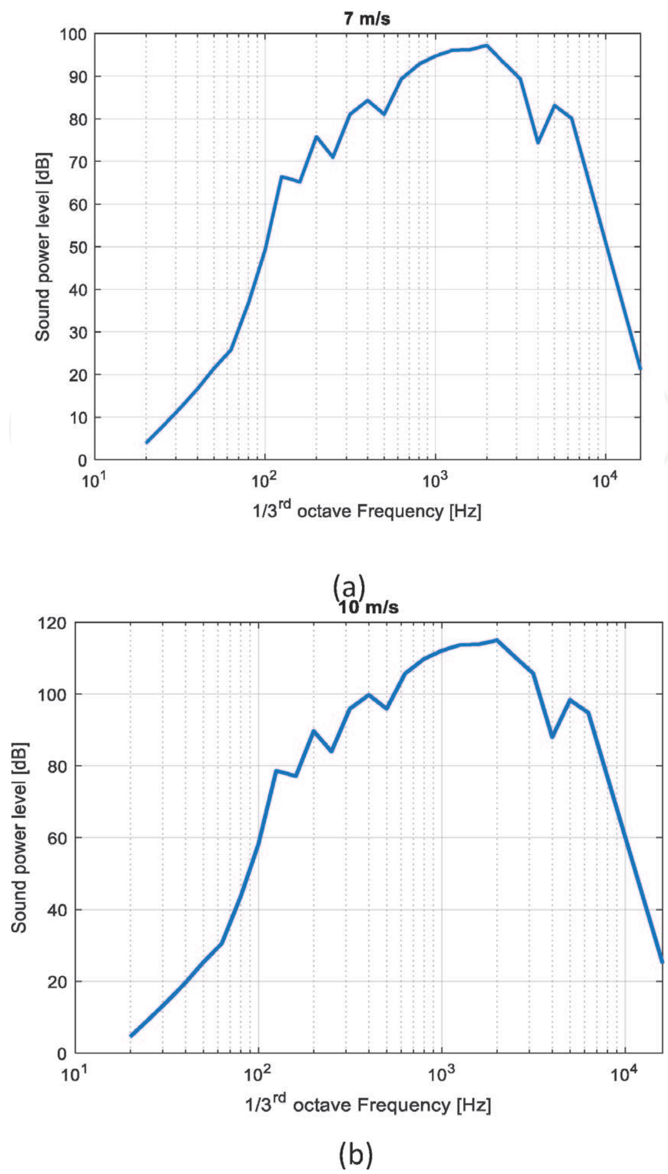

Figure 11.
Computed turbulent boundary layer vortex shedding noise (TEB-VS) for a blade length of 38 m, 2 MW turbine using trailing edge thickness of 0.5%c at two different wind speeds (a) 7 m/s (b) 10 m/s.

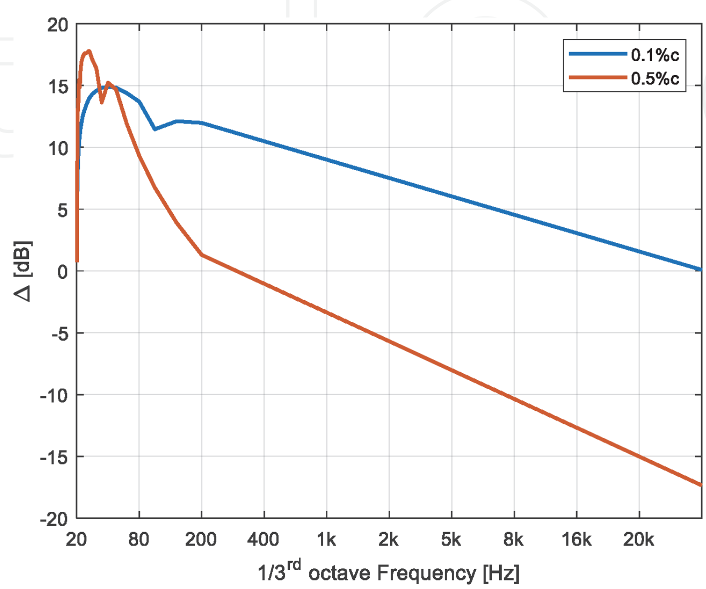

Figure 12.
Computed difference, Δ dB, of the turbulent boundary layer vortex shedding noise level (TEB-VS) between wind speeds 7 m/s and 10 m/s, at trailing edge thicknesses of 0.1%c and 0.5%c.

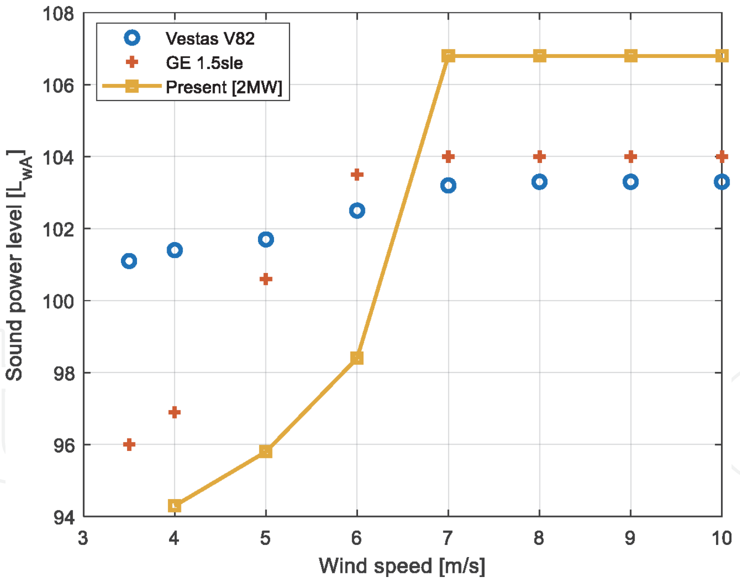

Figure 13.
Sound power levels computed for various wind speeds, for present 2 MW turbine, 38 m blade length compared to experiment data for Vestas V82, GE 1.5sle at same hub heights.

5. Conclusion

A computational analysis of trailing edge bluntness vortex shedding noise for 2 MW horizontal axis turbine was performed for trailing edge thicknesses of 0.1% and 0.5% local chord using original BPM model. The original BPM results for trailing edge bluntness noise showed that for a trailing edge thickness of 0.1% and 0.5% chord length the effect on sound power level was found to be ~83 dB, 92 dB and 95 dB and 115 dB at wind speeds of 7 m/s and 10 m/s respectively. At 10 kHz region turbulent boundary layer vortex shedding noise masks all other self-noise mechanisms. Finally, the existing overall sound power level (OSPL) experimental data showed very good agreement with simulated outputs for the trailing edge bluntness noise at wind speeds 7 m/s 8 m/s and 10 m/s respectively. The original BPM results for trailing edge bluntness noise showed that for a trailing edge thickness of 0.1% chord the effect on $1/3^{rd}$ octave overall A weighted sound level was found as a peak hump with an amplitude of ~90 dBA near 10 kHz region and masks all other self-noise mechanisms. The modified BPM results for trailing edge bluntness noise also showed a sharp peak instead of a hump but the amplitude reduced by ~15 dBA at 8 kHz in noise spectra. The new thickness correction function predicted the peak amplitude of trailing edge bluntness more accurately compared to original and modified BPM.

Conflict of interest

Authors declare no conflict of interest for the present work.

Nomenclature

M	Mach number
h/δ^*	Trailing edge bluntness ratio
δ^*	Boundary layer displacement thickness, mm
L	Length of span segment, m

r_e	Distance between the source and receiver position, m
G_4, G_5	Shape functions
θ, ϕ	Directivity angles between the source and receiver line
SPL	Sound power level, sound pressure level, dB
D_h	High frequency directivity
Ψ	Trailing edge angle, degree
K_o	Empirical constant
r	Local radius, m
R	Blade radius, m
t/c	thickness to chord ratio
L_{wA}	A -weighted sound power level
St'''	Strouhal number
HH	Hub height, m
D	Rotor diameter, m
St_{peak}'''	Peak Strouhal number
δ^*_{avg}	Average boundary layer displacement thickness, mm
M_c	Critical Mach number
f	Frequency, Hz
U	Free stream wind velocity, wind speed, m/s
c	Chord length

Author details

Satya Prasad Maddula[1], Vasishta Bhargava Nukala[2]*,
Swamy Naidu Neigapula Venkata[3], Chinmaya Prasad Padhy[4] and Rahul Samala[5]

1 Department of Aerospace Engineering, GITAM (Deemed to be University), Hyderabad, India

2 Department of Mechanical Engineering, Sreyas Institute of Engineering and Technology, Hyderabad, India

3 Department of Mechanical Engineering, NIT Raipur, Raipur, India

4 Department of Mechanical Engineering, GITAM (Deemed to be University), Hyderabad, India

5 Department of Applied Mechanics, Indian Institute of Technology, Chennai, India

*Address all correspondence to: vasishtab@gmail.com

References

[1] Bastasch M, van Dam J, Sondergaard B, Rogers A. Wind Turbine Noise – An Overview. Journal of Canadian Acoustical Association. 2006;**34**(2):7-16

[2] Geyer T, Sarradj E, Fritzsche C. Porous Aerofoils: Noise Reduction and Boundary Layer Effects. International Journal of Aeroacoustics. 2010;**9**(6): 787-820. DOI: 10.1260/1475-472X.9.6.787

[3] Tang H, Lei Y, Fu Y. Noise reduction mechanisms of an airfoil with trailing edge serrations at low Mach number. *MDPI*: *Applied science*; 2019 https://doi.org/10.3390/app9183784

[4] Kingan, K.M.*Aero-Acoustic Noise Produced by an Aerofoil* [Doctoral thesis]. Christchurch: University of Canterbury, New Zealand, 2005, p. 448. Available from: https://ir.canterbury.ac.nz/handle/10092/6596

[5] Brooks. T.F and Hodgson. T.H, Trailing Edge Noise Prediction from Measured Surface Pressures*. Journal of Sound and Vibration,* vol 78, p 69-117. 1981, DOI: https://doi.org/10.1016/S0022-460X(81)80158-7

[6] Brooks, T.F., Pope, D.S. and Marcolini, M.A, *Airfoil Self Noise and Prediction.* NASA reference publication 1218, 1989, Available from: https://ntrs.nasa.gov/archive/nasa/casi.ntrs.nasa.gov/19890016302.pdf

[7] Zhu WJ. *Modelling of Noise from Wind Turbines* [Master thesis]. Lyngby: Department of Wind Energy, Technical University of Denmark; 2004

[8] Moriarty, P. and Migliore, P.(2003) *Semi Empirical Aero-Acoustic Noise Prediction Code for Wind Turbines* [Technical report], 2003, 39 p. Available from:http://citeseerx.ist.psu.edu/viewdoc/download?doi=10.1.1.197.1153&rep=rep1&type=pdf

[9] Wei, Z. J; Shen, W.Z; Sorensen, J.N; Leloudas, G (2016) Improvement of airfoil trailing edge bluntness noise model, *Advances in mechanical engineering* , 2016, vol 8, p 1-12, DOI: 10.1177/1687814016629343

[10] Grosveld FW. Prediction of Broadband Noise from Horizontal Axis Wind Turbines. Journal of Propulsion and Power. 1985;**1**(4):292-299 ISSN 0748-4658

[11] Howe. M. S *Theory of Vortex Sound* Cambridge University Press. 2003, DOI: https://doi.org/10.1017/CBO9780511755491

[12] Doolan C, Moreau DJ, Arcondoulis E, Albarracin C. Trailing Edge Noise Production. Prediction and Control. *New Zealand Acoustics*. 2012; **25**(3):22-29

[13] Blandeau, V.P and Joseph, P.F, Validity of Amiet's Model for Propeller Trailing Edge Noise. AIAA Journal, 2011, vol. 49, no 5, p. 1057-1066. DOI 10.2514/1.J050765.

[14] Dijkstra, P, *Rotor Noise and Aero-Acoustic Optimization of Wind Turbine Aerofoils* [Master Thesis]. Delft: Delft University of Technology. 131 p. 2015.

[15] Leloudas, G, *Optimization of Wind Turbines with Respect to Noise* [Master Thesis]. Lyngby: Technical University of Denmark, p. 66, 2006.

[16] Blake, W.K, *Aero-Hydro-Acoustics for Ships Volume II*, [Technical Report] 1984. Available from: https://apps.dtic.mil/dtic/tr/fulltext/u2/a150672.pdf

[17] Moreau, D.J, Brooks, L. A. and Doolan, C, Flat Plate Self-Noise Reduction at Low to Moderate Reynolds Number with Trailing Edge Serrations. In *Proceedings of Acoustics.* Gold Coast: Australia. 2011, Available from: https://

pdfs.semanticscholar.org/74fa/0f9f258c0d5c5a1f846abb244c6d7505b213.pdf

[18] NuMAD software, Version: NuMADexe_130403_PCWIN64. Available from: https://energy.sandia.gov/energy/renewable-energy/wind-power/rotor-innovation/numerical-manufacturing-and-design-tool-numad.

[19] Bhargava V, Maddula SP, Samala R. Prediction of vortex induced aerodynamic noise from wind turbine blades. Advances in Military Technology. 2019;**14**(p):245-261. DOI: 10.3849/aimt.01295

[20] Appendix 1, Environmental sound survey and noise impact assessment, *Draft Environmental Impact Assessment, Jericho Rise Wind Farm LLC. TetraTech EC Inc, Boston, USA, 2008.*

[21] Lowson, M. V., Assessment and Prediction of Wind Turbine Noise, Flow Solutions Report 92/19, ETSU W/13/00284/REP, pp. 1-59, 1992.

[22] Hau E, Langenbrinck J. Palz, W. Springer-Verlag, Berlin: WEGA Large wind turbines; 1993. pp. 1-143

[23] Hagg, F., van der Borg., N. J. C.M Bruggeman, J. C.; et al. Definite Aero-Geluidonderzoek Twin," Stork Product Engineering B.V., SPE 92- 025. 1992.